



This is the accepted manuscript made available via CHORUS. The article has been published as:

Demonstration of a Bosonic Quantum Classifier with Data Reuploading

Takafumi Ono, Wojciech Roga, Kentaro Wakui, Mikio Fujiwara, Shigehito Miki, Hiroataka Terai, and Masahiro Takeoka

Phys. Rev. Lett. **131**, 013601 — Published 6 July 2023

DOI: [10.1103/PhysRevLett.131.013601](https://doi.org/10.1103/PhysRevLett.131.013601)

Demonstration of a bosonic quantum classifier with data re-uploading

Takafumi Ono^{1,2,*}, Wojciech Roga^{3,†}, Kentaro Wakui⁴, Mikio Fujiwara⁴, Shigehito Miki⁵, Hirotaka Terai⁵, and Masahiro Takeoka^{3‡}

¹*Program in Advanced Materials Science Faculty of Engineering and Design, Kagawa University, 2217-20 Hayashi-cho, Takamatsu, Kagawa 761-0396, Japan*

²*JST, PRESTO, 4-1-8 Honcho, Kawaguchi, Saitama 332-0012, Japan*

³*Department of Electronics and Electrical Engineering, Keio University, 3-14-1 Hiyoshi, Kohoku-ku, Yokohama 223-8522, Japan*

⁴*Advanced ICT Research Institute, National Institute of Information and Communications Technology (NICT), Koganei, Tokyo 184-8795, Japan and*

⁵*Advanced ICT Research Institute, National Institute of Information and Communications Technology, 588-2 Iwaoka, Nishi, Kobe 651-2492, Japan*

(Dated: May 31, 2023)

In a single qubit system, a universal quantum classifier can be realized using the data re-uploading technique. In this study, we propose a new quantum classifier applying this technique to bosonic systems and successfully demonstrate it using a silicon-based photonic integrated circuit. We established a theory of quantum machine learning algorithm applicable to bosonic systems and implemented a programmable optical circuit combined with an interferometer. Learning and classification using part of the implemented optical quantum circuit with uncorrelated two-photons resulted in a classification with a success probability of $94 \pm 0.8\%$ in the proof of principle experiment. As this method can be applied to an arbitrary two-mode N-photon system, further development of optical quantum classifiers, such as extensions to quantum entangled and multi-photon states, is expected in the future.

Recently, there has been a lot of work on quantum machine learning algorithms that can apply machine learning methods to quantum systems in a sophisticated and efficient manner [1–8]. Among quantum machine learning algorithms, classifiers belong to the supervised learning category and classify the input data into certain categories (classes) [9–11]. It is particularly effective when the correct or optimal solution to a problem is known for training data. Usually, quantum classification consists of three steps: encoding of the data into the quantum state, processing, and measurement, whereby the parameters characterising the classifier are adjusted to build a classification model. Various quantum classifiers have been proposed, using quantum circuit models based on qubits [9, 12] and neural network-like models based on bosonic systems [13–16]. Moreover, optical quantum classifiers harnessing entanglement have been demonstrated in [17] targeting, if appropriately scaled, potential exponential speed-up of high dimensional data classification. In particular, the properties of these classifiers strongly depend on the data encoding method, and their performance depends on the number of qubits in the quantum circuits or the number of neurons in the hidden layer in the neural network, indicating that implementing higher-performance classifiers requires complex quantum circuits or networks [18, 19].

Among the bosonic quantum circuit, silicon-based optical integrated circuits have the advantages of high integration density, sophisticated fabrication techniques in their mature stage of technology development and low op-

tical losses in the communication wavelength band [20]. In particular, this platform works well with CMOS electronics, allowing light to propagate on a waveguide while the quantum state of light is controlled by electrical circuits. There have been reports of on-chip quantum entangled state generation and measurement [21], as well as the realization of an optical interferometer operating with extinction ratios exceeding approximately 60 dB [22], and the performance of each device has been improved [23]. The reason behind these developments of optical quantum-integrated circuits is that it is feasible to construct programmable optical quantum circuits by combining multiple stages of interferometers [24–26]. For these reasons, research into the application of programmable optical quantum circuits has intensified recently [27].

Typical schemes of quantum classifiers tend to adopt the amplitude encoding of the classical or quantum data into input quantum states. However, implementation of this strategy in the integrated photonics could be limited so far for a few reasons: this method requires a larger number of photons or modes to create Hilbert spaces of appropriate sizes, and the non-linearity obtained in this method is limited. The breakthrough seems to be proper adaptation of the so-called data re-uploading technique recently introduced for qubit-based circuits in [28]. In this paper the authors demonstrate a universal quantum classifier of classical data using a single qubit circuit with repeated data re-uploading in different parts of the circuit. In this method, the unitary transformation repre-

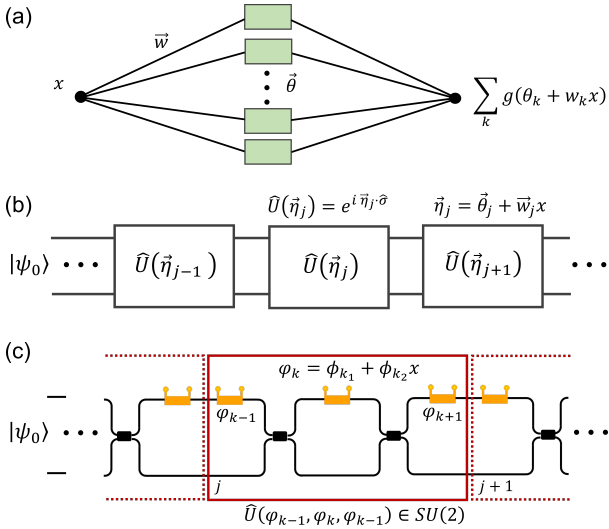


FIG. 1. (a) A scheme of a single-layer neural network characterized by neurons with weights \vec{w} , biases $\vec{\theta}$, and a sigmoid activation function g . If the number of neurons is sufficiently large, the output signal can approximate arbitrary function of data x . (b) Scheme of two-mode optical system realizing the data re-uploading scheme of a universal classifier. It consists of unitary transformation characterized by parameters $\vec{\eta}_j$ that depend on data x and adjustable parameters \vec{w}_j and $\vec{\theta}_k$. (c) The realistic optical data re-uploading classifier that can be realized on a silicon chip. The unitary encircled by the solid frame can realize arbitrary $SU(2)$ transformation.

senting the quantum circuit is divided into multiple layers, and data-encoding and training are repeatedly performed in each layer. It has been shown that a universal quantum classifier can be realized with a single qubit by increasing the number of layers of the circuit instead of increasing the number of qubits. Moreover, the same concept of multi-qubit circuits with possible entangled states leads to the conclusion that systems with entanglement seem to perform better.

As we will show in this paper, the data re-uploading technique is applicable to qubit systems as well as bosonic systems implemented on silicon photonics even with a single photon that manifests remarkable computational power when used in an appropriate bosonic quantum circuit. This motivated us to leverage the advantages of integrated photonics mentioned above to develop a quantum classifier [29].

In this letter, we report on the experimental realization of a universal bosonic quantum classifier using silicon photonic circuits. We have applied the idea of a data re-uploading method proposed for qubit systems to bosonic quantum systems and implemented it using programmable integrated photonic circuits. As a proof-of-principle experiment, we built a bosonic system consisting of a three-layer two-mode circuit and two-photon input state. For the optimization of the circuit parameters, we use the sequential minimal optimization method,

which has been proposed recently [30]. By training a part of the circuit, we have successfully classified points divided by an elliptical boundary with a success probability of $94 \pm 0.8\%$. This work is expected to lead to further progress in optical quantum classifiers based on bosonic systems using quantum entangled and multi-photon states.

The universality of a single qubit processor relies on properties of the $SU(2)$ group unitary transformations used in the circuit [28], figure 1. The group can be naturally parameterised by coefficients $\vec{\eta}$ in front of Pauli matrices $\vec{\sigma}$ which are the group generators, i.e., $\hat{U}(\vec{\eta}) = e^{i\vec{\eta}\vec{\sigma}}$. Concatenation of two elements of $SU(2)$, $\hat{U}(\vec{\eta}_1)$ and $\hat{U}(\vec{\eta}_2)$ stays in the group, but its parameterisation is in general a non-linear function ω of the coefficients of the parts, $\hat{U}(\vec{\eta}_1)\hat{U}(\vec{\eta}_2) = \hat{U}(\omega(\vec{\eta}_1, \vec{\eta}_2))$. Reference [28] shows that using concatenation of many unitary transformations the parameters of which depend on the data x as $\vec{\eta}_i = \vec{\theta}_i + \vec{w}_i x$, one can achieve the transformation with parameterization $\hat{U}(\sum_i f(\vec{\theta}_i + \vec{w}_i x))$, with a nonlinear function f . According to the universal approximation theory for single layer neural networks, figure 1 (a), the argument of this \hat{U} , figure 1 (b), can approximate arbitrary function. Namely, transformations by \hat{U} and functions of its elements could be substantial to realize desired computational tasks when sufficiently long circuit with data re-uploading is prepared. In the two-mode bosonic circuit, any $SU(2)$ transformation can be realized by passive elements and can define an input-output relation between mode-creation operators. Therefore, the reasoning that leads to achievability of $\hat{U}(\sum_i f(\vec{\theta}_i + \vec{w}_i x))$ holds in this context as well. Also in this case, the measurement leads to functions of the entries of the final \hat{U} , therefore the computational power of the two mode bosonic processor is at least the same that of the one-qubit processor. This suggests that two-mode circuits with multiple photons may provide some computational advantages.

Here we adopted the data re-uploading method by [28] to bosonic system of the photonic quantum circuit. A scheme is shown in figure 1 where we indicate the analogy between two-mode optical circuit and a classical single-layer neural network. According to the universal approximation theory, it can approximate an arbitrary function of the input data x by its output signal $\sum_k g(\theta_k + w_k x)$. Here, g is usually a sigmoid function, \vec{w} is a vector of weights and $\vec{\theta}$ is a vector of biases. In our implementation (figure 1. (c)) variables have been changed from $\vec{\eta}_j$ used in the universality argument to the phases of the phase shifters $\varphi_k = \phi_{k_1} + \phi_{k_2} x^{(i)}$ which are directly modified in practice. The data re-uploading method decomposes the unitary operation of an optical quantum circuit into multiple sequential layers of unitary transformations. In practice we use the following decomposition

$$\hat{U}(\vec{\phi}, \vec{x}^{(i)}) = \hat{U}_{BS} \hat{V}_1(\varphi_1) \hat{U}_{BS} \dots \hat{V}_N(\varphi_N) \hat{U}_{BS}, \quad (1)$$

where $\varphi_k = \phi_{k_1} + \phi_{k_2} x^{(i)}$, \hat{V}_i denotes a phase-shifter, and

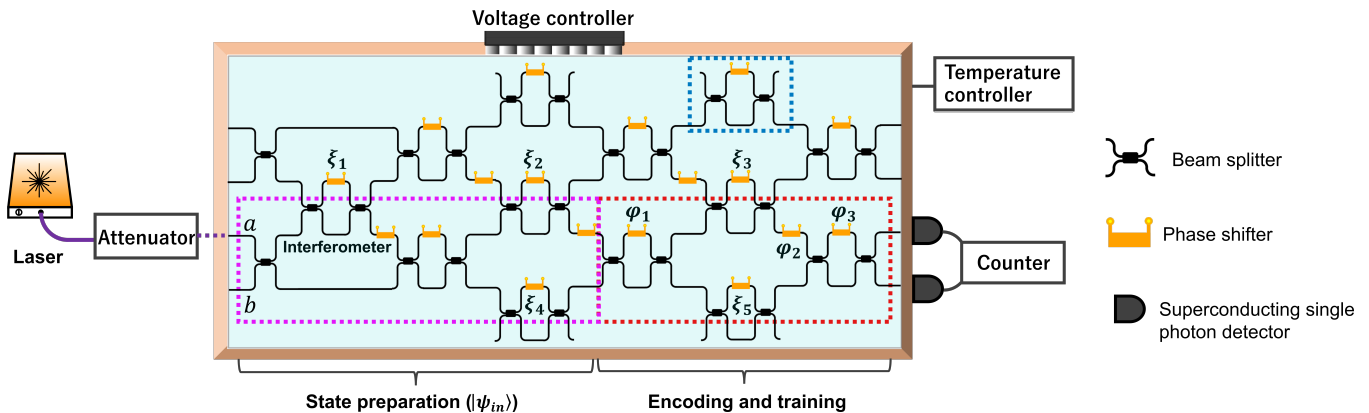


FIG. 2. Schematic of the implemented optical quantum circuit. The first stage generates an arbitrary quantum state. The parameters for data and tuning are encoded into the parameters of the unitary transformation in the latter stage of the optical quantum circuit.

\hat{U}_{BS} denotes the 50:50 beam splitter. Here the index i indicates one of the data points. Parameters, φ_k , in the transformations depend on specific free parameters, ϕ_k , and the same data applied in each \hat{V}_i . We define an arbitrary quantum state as $|\psi_{in}\rangle$ that is the input state of this quantum circuit. The input data $\{\vec{x}^{(i)}\}$ to be classified are encoded into the parameters of the unitary operations of the circuit. Classification is then realized by optimizing the free parameters of each unitary operation. The unitary operation for encoding and tuning is therefore a function of the input data $\{\vec{x}^{(i)}\}$ and the tuning parameters $\vec{\phi}$ as given by $\hat{U}(\vec{\phi}, \vec{x}^{(i)})$. Finally, the probability $p^{(i)}(\vec{\phi}) = \left| \langle m | \hat{U}(\vec{\phi}, \vec{x}^{(i)}) | \psi_{in} \rangle \right|^2$ of obtaining a particular output m is measured. At this point, a threshold value is set and the data is classified. For example, the point \vec{x}_i is classified as "yes" if the probability $p^{(i)}(\vec{\phi})$ is higher than the threshold value and "no" if it is lower. The tuning parameters $\vec{\phi}$ of the training optical quantum circuits are optimized so that the least square error cost function

$$C(\vec{\phi}) = \sum_i \left(p^{(i)}(\vec{\phi}) - y^{(i)} \right)^2, \quad (2)$$

is as small as possible. Here $y^{(i)}$ is the classification of the training data, $y^{(i)} \in \{0, 1\}$.

In the training process of adjusting free parameters of the circuit, we apply a modification of gradient descent algorithm [31], so-called Sequential Minimal Optimization (SMO) introduced in [30] adapted to our photonic set up [32]. This approach, which relies on analytical minimization of the cost function, works more efficiently under certain constraints than other numerical methods such as the gradient method [30]. It is easy to implement in optical systems like ours where only one type of transformation, i.e., the phase shifter, is optimized. In this case, the complexity of the method per parameter scales with the number of photons, not with the number

of modes, or the particular structure of the circuit [32].

The encoding of the input and optimization of the tuning parameters are repeatedly performed in each phase-shift transformation. Note that in this implementation, encoding of the input data into the quantum state and tuning of the circuit are performed simultaneously. The optical quantum circuit was optimized so that the cost function is as small as possible by repeating this step several times, with the optimization of all parameters $\vec{\phi}$ as a single step. In quantum circuit models, it has been shown that the value of the cost asymptotically approaches a minimum value when the number of steps is repeated [28], but the asymptotics of the minimum value in bosonic systems is a subject for future research.

We have implemented the quantum machine learning algorithm using a silicon-based photonic integrated circuit. A scheme of the circuit is shown in figure 2. The optical quantum circuit consists of four inputs and four outputs and combines an interferometer with phase shifters to realize a programmable optical quantum circuit [33]. Control of the phase of the light was achieved by applying voltage to a thermal resistive element placed above the optical waveguide and locally applying heat to change the refractive index of the silicon optical waveguide. Note that some additional interferometers have been added to ensure proper alignment of the phase-shifter inside the circuit (e.g., the interferometer surrounded by the blue line in the circuit). The interferometers in figure 2 were evaluated using laser light and the extinction ratio was measured to be more than 30 dB for all interferometers.

In this proof-of-principle experiment, we used two spatial modes of the circuit (enclosed by the purple and red dotted line in figure 2) for an optical quantum classifier. To do this, we set the bias phases ($\xi_1, \xi_2, \xi_3, \xi_4, \xi_5$) of the interferometers to 0 so that these interferometers act as straight waveguide. As an input state, we produced an uncorrelated two-mode two-photon state, $|2; 0\rangle$, from the attenuated input laser by post-selection. Several beam

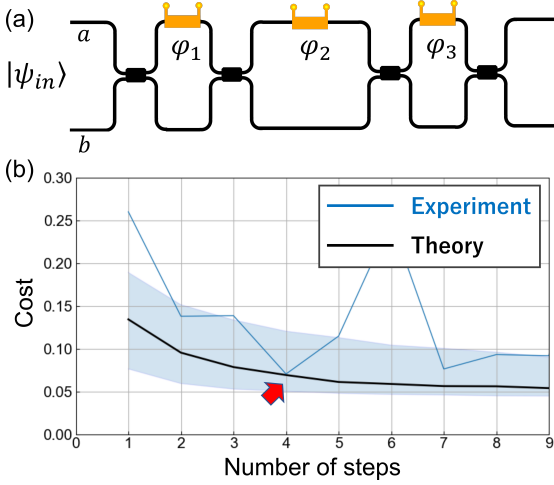


FIG. 3. (a) Schematic of the photon circuit used. The circuit shown in the red box in Fig. 2(a) is decomposed into three layers. (b) Value of the cost at each step, optimized using the data reuploading technique. The black line is the theoretical value and the blue line is the experimental value. The theoretical values are the average of the values optimized by simulation using 200 training data (3000 times). The region between the 10th and 90th percentile is shown in semi-transparent blue.

splitters and phase-shifters are placed before the proper circuit, and these elements are used to implement the linear optical unitary operation \hat{U} . The resulting quantum state input to the classifier is $|\psi_{in}\rangle = \hat{U}|2;0\rangle$. Since the data re-uploading method in this study is valid for any two-mode two-photon input state, the \hat{U} is irrelevant (it can be inverted by the proper part of the circuit).

A simplified quantum circuit for encoding and training is shown in figure 3 (a). The quantum circuit consists of three unitaries given by $\hat{V}_1(\varphi_1)$, $\hat{V}_2(\varphi_2)$, and $\hat{V}_3(\varphi_3)$ and 50:50 beam splitters. We used the two-dimensional data as $\vec{x}^{(i)} = (x_1^{(i)}, x_2^{(i)})$ to be classified. Data $\vec{x}^{(i)}$ and tuning parameters $\vec{\phi} = \{\phi_1, \phi_2, \phi_3, \phi_4, \phi_5, \phi_6\}$ are encoded into the parameters of the unitaries as follows,

$$\begin{aligned}\varphi_1 &= \phi_1 + \phi_2 \times x_2^{(i)} \\ \varphi_2 &= \phi_3 + \phi_4 \times x_1^{(i)} \\ \varphi_3 &= \phi_5 + \phi_6 \times x_2^{(i)}.\end{aligned}\quad (3)$$

The output quantum state in this type of experiment with three layers is therefore given by

$$|\psi_{out}\rangle = \hat{U}_{BS}\hat{V}_3(\varphi_3)\hat{U}_{BS}\hat{V}_2(\varphi_2)\hat{U}_{BS}\hat{V}_1(\varphi_1)\hat{U}_{BS}|\psi_{in}\rangle.\quad (4)$$

and can be easily extended to more complicated configurations. The measurements were performed with one photon output for each spatial mode for each photon ($\langle m|_{ab} = \langle 1;1|_{ab}$). As a result, the probability obtained at the output of the optical quantum circuit is given by

$$p(\vec{\phi}, \vec{x}) = |\langle 1;1|\psi_{out}\rangle|^2.\quad (5)$$

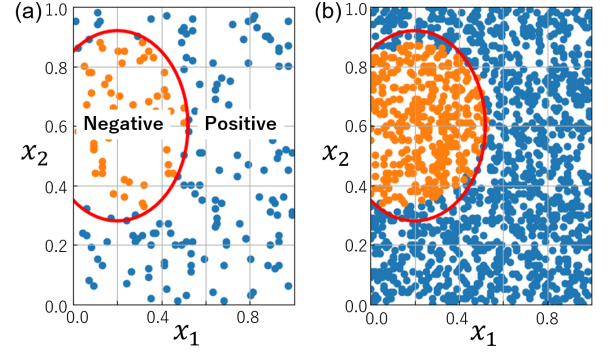


FIG. 4. (a) The area to be classified in the light quantum circuit is shown. Red lines are the boundaries of the regions to be divided. (b) Classification results. Yellow dots are teacher data belonging to negative regions, blue dots are teacher data belonging to positive regions.

For a given 2D function, the tuning parameters $\vec{\phi} = (\phi_1, \phi_2, \phi_3, \phi_4, \phi_5, \phi_6)$ are optimized so that the cost given by equation (2) becomes as small as possible. In this study, we find an explicit formula for $p(\vec{\phi}, \vec{x}^{(i)})$ for each ϕ_j in each step of the training by using the SMO instead of minimizing the cost numerically by gradient descent [32].

In this experiment, we chose the circle specified by x_1 and x_2 as the classification border function,

$$(x_1 - 0.2)^2 + (x_2 - 0.6)^2 = 0.32^2.\quad (6)$$

The classification was then carried out with training data points inside this circle classified as $y^{(i)} = 0$ and points outside this circle classified as $y^{(i)} = 1$. The number of training data points was 200, and the parameter $\vec{\phi}$ was optimized to keep the cost as low as possible using our SMO. Figure 3 (b) shows the optimal value of the cost at each step. The black line represents the results from theoretical simulations; the blue lines is experimental values. Theoretical simulations confirm that the cost decreases monotonically at each step, as expected. However, in the experiments, there was a tendency for costs to increase at certain steps, so the classification was carried out under the condition that corresponds to the lowest costs. The jump is caused by the instability of the numerical minimization algorithm used to find the minimum of the cost function along a single variable.

Figure 4 shows the results of classification on 1500 data points using the trained optical quantum circuit. It can be visually confirmed that the classification was correct. Quantitatively, we obtained true positive (TP) and false negative (FN) values as 1085 and 10, respectively. We also obtained false positive (FP) and true negative (TN) as 45 and 360, respectively. We then calculated true pos-

itive rate (TPR) and true negative rate (TNR) as

$$TPR = \frac{TP}{TP + FN} = 99.1 \pm 0.3\%,$$

$$TNR = \frac{TN}{TN + FP} = 88.9 \pm 1.6\%. \quad (7)$$

Thus, on average, the classification was confirmed to be correct with a success probability of approximately $94.0 \pm 0.8\%$. Here, errors are standard deviations calculated by error propagation, assuming that TP, FN, TN, and FP counts follow the Poissonian distribution.

In conclusion, we have applied the universal quantum classifier method proposed for qubit systems to optical quantum circuits in bosonic systems. Specifically, the unitary transformation of the optical quantum circuit was decomposed into multiple layers allowing for implementation of the data re-uploading technique. In each layer, the data and tuning parameters were encoded into the unitary transformation. Machine learning techniques were then used to optimize costs. We implemented the proposed optical quantum classifier by using a silicon-based photonic integrated circuit. The input quantum states are uncorrelated two-mode two-photon states. 200 training data points were used to train the optical quantum circuit. Finally, we performed classification on 1500 test data, the quantum classifier was implemented with a success probability of approximately $94 \pm 0.8\%$. Although the quantum states used in this study are not entangled, entanglement based quantum classifiers can be implemented on the same circuit. Based only on the fact that entangled states occupy a significant volume of the set of all quantum states of a given dimensionality of the Hilbert space [34] we expect that the classifiers that allow for entanglement may perform better than classifiers without entanglement at least for some problems with finite-length classifiers as shown in [32]. Other evidence were provided in [28]. In general, we have shown that the universal quantum classifier with data re-uploading method proposed for qubit systems can be naturally applied to boson-based optical quantum circuits. In the future, it is expected that increasing the number of spatial modes and the number of photons will lead to higher-performance quantum classifiers.

Acknowledgements This work was supported by JST PRESTO Grant No. JPMJPR1864, The Murata Science Foundation, JST CREST Grant No. JPMJCR1772, and JST Grant No. JPMJPF2221.

* ono.takafumi@kagawa-u.ac.jp

† wojciech.roga@keio.jp

‡ takeoka@elec.keio.ac.jp

[1] G. D. Paparo, V. Dunjko, A. Makmal, M. A. Martin-Delgado, and H. J. Briegel, *Physical Review X* **4**, 031002 (2014).

- [2] I. M. Georgescu, S. Ashhab, and F. Nori, *Reviews of Modern Physics* **86**, 153 (2014).
- [3] N. C. Harris, G. R. Steinbrecher, M. Prabhu, Y. Lahini, J. Mower, D. Bunandar, C. Chen, F. N. Wong, T. Baehr-Jones, M. Hochberg, S. Lloyd, and D. Englund, *Nature Photonics* **11**, 447 (2017).
- [4] J. Biamonte, P. Wittek, N. Pancotti, P. Rebentrost, N. Wiebe, and S. Lloyd, *Nature* **549**, 195 (2017).
- [5] Y. Shen, N. C. Harris, S. Skirlo, M. Prabhu, T. Baehr-Jones, M. Hochberg, X. Sun, S. Zhao, H. Larochelle, D. Englund, and M. Soljacic, *Nature Photonics* **11**, 441 (2017).
- [6] S. Yu, F. Albarrán-Arriagada, J. C. Retamal, Y. T. Wang, W. Liu, Z. J. Ke, Y. Meng, Z. P. Li, J. S. Tang, E. Solano, L. Lamata, C. F. Li, and G. C. Guo, *Advanced Quantum Technologies* **2**, 1800074 (2019).
- [7] S. Lloyd, M. Schuld, A. Ijaz, J. Izaac, and N. Killoran, arXiv:2001.03622 (2020).
- [8] R. Sweke, J. P. Seifert, D. Hangleiter, and J. Eisert, *Quantum* **5**, 417 (2021).
- [9] K. Mitarai, M. Negoro, M. Kitagawa, and K. Fujii, *Physical Review A* **98**, 032309 (2018).
- [10] M. Schuld, A. Bocharov, K. M. Svore, and N. Wiebe, *Physical Review A* **101**, 032308 (2020).
- [11] S. Y. C. Chen, C. M. Huang, C. W. Hsing, and Y. J. Kao, *Machine Learning: Science and Technology* **2**, 045021 (2021).
- [12] V. Havlíček, A. D. Córcoles, K. Temme, A. W. Harrow, A. Kandala, J. M. Chow, and J. M. Gambetta, *Nature* **567**, 209 (2019).
- [13] M. Lewenstein and M. Olko, *Network: Computation in Neural Systems* **2**, 207 (1991).
- [14] P. Rebentrost, T. R. Bromley, C. Weedbrook, and S. Lloyd, *Physical Review A* **98**, 042308 (2018).
- [15] G. R. Steinbrecher, J. P. Olson, D. Englund, and J. Carolan, *npj Quantum Information* **5**, 60 (2019).
- [16] I. Cong, S. Choi, and M. D. Lukin, *Nature Physics* **15**, 1273 (2019).
- [17] X.-D. Cai, D. Wu, Z.-E. Su, M.-C. Chen, X.-L. Wang, L. Li, N.-L. Liu, C.-Y. Lu, and J.-W. Pan, *Phys. Rev. Lett.* **114**, 110504 (2015).
- [18] M. Cerezo, A. Arrasmith, R. Babbush, S. C. Benjamin, S. Endo, K. Fujii, J. R. McClean, K. Mitarai, X. Yuan, L. Cincio, and P. J. Coles, *Nature Reviews Physics* **3**, 625 (2021).
- [19] M. Schuld, R. Sweke, and J. J. Meyer, *Physical Review A* **103**, 032430 (2021).
- [20] D. Thomson, A. Zilkie, J. E. Bowers, T. Komljenovic, G. T. Reed, L. Vivien, D. Marris-Morini, E. Cassan, L. Virost, J.-M. Fédéli, J.-M. Hartmann, J. H. Schmid, D.-X. Xu, F. Boeuf, P. O'Brien, G. Z. Mashanovich, and M. Nedeljkovic, *Journal of Optics* **18**, 073003 (2016).
- [21] F. Raffaelli, G. Ferranti, D. H. Mahler, P. Sibson, J. E. Kennard, A. Santamato, G. Sinclair, D. Bonneau, M. G. Thompson, and J. C. Matthews, *Quantum Science and Technology* **3**, 025003 (2018).
- [22] C. M. Wilkes, X. Qiang, J. Wang, R. Santagati, S. Paesani, X. Zhou, D. A. B. Miller, G. D. Marshall, M. G. Thompson, and J. L. O'Brien, *Optics Letters* **41**, 5318 (2016).
- [23] J. F. Tasker, J. Frazer, G. Ferranti, E. J. Allen, L. F. Brunel, S. Tanzilli, V. D'Auria, and J. C. Matthews, *Nature Photonics* **15**, 11 (2021).
- [24] M. Tillmann, B. Dakić, R. Heilmann, S. Nolte, A. Sza-

- meit, and P. Walther, *Nature Photonics* **7**, 540 (2013).
- [25] X. Qiang, X. Zhou, J. Wang, C. M. Wilkes, T. Loke, S. O’Gara, L. Kling, G. D. Marshall, R. Santagati, T. C. Ralph, J. B. Wang, J. L. O’Brien, M. G. Thompson, and J. C. Matthews, *Nature Photonics* **12**, 534 (2018).
- [26] S. Paesani, Y. Ding, R. Santagati, L. Chakhmakhchyan, C. Vigliar, K. Rottwitt, L. K. Oxenløwe, J. Wang, M. G. Thompson, and A. Laing, *Nature Physics* **15**, 925 (2019).
- [27] J. Wang, F. Sciarrino, A. Laing, and M. G. Thompson, *Nature Photonics* **14**, 273 (2020).
- [28] A. Pérez-Salinas, A. Cervera-Lierta, E. Gil-Fuster, and J. I. Latorre, *Quantum* **4**, 226 (2020).
- [29] J. Carolan, C. Harrold, C. Sparrow, E. Martín-López, N. J. Russell, J. W. Silverstone, P. J. Shadbolt, N. Matsuda, M. Oguma, M. Itoh, G. D. Marshall, M. G. Thompson, J. C. Matthews, T. Hashimoto, J. L. O’Brien, and A. Laing, *Science* **349**, 711 (2015).
- [30] K. M. Nakanishi, K. Fujii, and S. Todo, *Physical Review Research* **2**, 043158 (2020).
- [31] R. Sweke, F. Wilde, J. J. Meyer, M. Schuld, P. K. Fährmann, B. Meynard-Piganeau, and J. Eisert, *Quantum* **4**, 314 (2020).
- [32] T. Ono, W. Roga, K. Wakui, M. Fujiwara, S. Miki, H. Terai, and M. Takeoka, *Supplementary information* (2022).
- [33] W. R. Clements, P. C. Humphreys, B. J. Metcalf, W. S. Kolthammer, and I. A. Walmsley, *Optica* **3**, 1460 (2016).
- [34] K. Życzkowski, P. Horodecki, A. Sanpera, and M. Lewenstein, *Physical Review A* **58**, 883 (1998).